

CHCA-1 is a copper-regulated CTR1 homolog required for normal development, copper accumulation, and copper-sensing behavior in *Caenorhabditis elegans*

Received for publication, April 26, 2018. Published, Papers in Press, May 21, 2018. DOI 10.1074/jbc.RA118.003503

✉ Sai Yuan[‡], Anuj Kumar Sharma^{‡1}, Alexandria Richart[‡], Jaekwon Lee[§], and Byung-Eun Kim^{‡¶2}

From the [‡]Department of Animal and Avian Sciences and [¶]Biological Sciences Graduate Program, University of Maryland, College Park, Maryland 20742 and the [§]Redox Biology Center, Department of Biochemistry, University of Nebraska, Lincoln, Nebraska 68588

Edited by Joseph M. Jez

Copper plays key roles in catalytic and regulatory biochemical reactions essential for normal growth, development, and health. Dietary copper deficiencies or mutations in copper homeostasis genes can lead to abnormal musculoskeletal development, cognitive disorders, and poor growth. In yeast and mammals, copper is acquired through the activities of the CTR1 family of high-affinity copper transporters. However, the mechanisms of systemic responses to dietary or tissue-specific copper deficiency remain unclear. Here, taking advantage of the animal model *Caenorhabditis elegans* for studying whole-body copper homeostasis, we investigated the role of a *C. elegans* CTR1 homolog, CHCA-1, in copper acquisition and in worm growth, development, and behavior. Using sequence homology searches, we identified 10 potential orthologs to mammalian CTR1. Among these genes, we found that *chca-1*, which is transcriptionally up-regulated in the intestine and hypodermis of *C. elegans* during copper deficiency, is required for normal growth, reproduction, and maintenance of systemic copper balance under copper deprivation. The intestinal copper transporter CUA-1 normally traffics to endosomes to sequester excess copper, and we found here that loss of *chca-1* caused CUA-1 to mislocalize to the basolateral membrane under copper overload conditions. Moreover, animals lacking *chca-1* exhibited significantly reduced copper avoidance behavior in response to toxic copper conditions compared with WT worms. These results establish that CHCA-1-mediated copper acquisition in *C. elegans* is crucial for normal growth, development, and copper-sensing behavior.

Copper is a crucial micronutrient involved in a wide range of catalytic reactions. It serves as a cofactor in cuproenzymes necessary for mitochondrial ATP synthesis, redox reactions, iron homeostasis, and neuropeptide biogenesis (1, 2). Given its

redox properties, copper accumulation can also be toxic to organisms due to generation of reactive oxygen species (1, 3). Organisms have adopted conserved copper homeostatic mechanisms to regulate copper uptake, detoxification, and distribution at both the cellular and systemic levels.

The intestinal epithelium is the main site for dietary copper absorption. Following reduction from Cu(II) to Cu(I) by a metallo-reductase, copper enters cells via the high-affinity copper transporter 1 (CTR1). Several metallochaperones such as CCS, COX17, and ATOX1 then deliver copper to Cu,Zn-superoxide dismutase (SOD1), cytochrome *c* oxidase, and ATP7A/ATP7B, respectively. ATP7A and ATP7B are P-type ATPases that transport copper to copper-dependent enzymes in the secretory pathway and export copper out of the cell. Upon export from the basolateral membrane of intestinal cells by ATP7A, copper is delivered to the liver, the main copper storage tissue, and other peripheral tissues as needed (1, 4).

The first copper transporter gene (*CTR*) was found in yeast, leading to the discovery of several CTR family members in humans, mice, fruit flies, and other species by homology searches and functional complementary studies (5). Although CTR proteins mediate copper uptake, they are expressed in different tissues during distinct developmental stages or as determined by copper availability. All characterized CTR proteins contain three putative transmembrane domains (TMD)³ with a Met-Xaa₃-Met domain in the second TMD. Electron crystallography revealed that human CTR1 (hCTR1) formed trimers at the plasma membrane (6–8). The extracellular N-terminal Met-rich domain, the Met-Xaa₃-Met motif, and the cytosolic C-terminal domain, Cys-His-Cys motif, are potential copper-binding sites necessary for effective copper transport (9–11). CTR1 localizes to the plasma membrane and intracellular vesicles, and its protein stability is regulated by copper at the post-translational level (12, 13). Human CTR2 facilitates truncation of the CTR1 ectodomain via a cathepsin protease (14, 15). Copper-dependent regulation of copper importers also occurs at the transcriptional level as *Saccharomyces cerevisiae* Ctr1 and Ctr3

This work was supported in part by National Institutes of Health Grants DK110195 (to B.-E. K.) and DK079209 (to J. L.) and Nebraska Redox Biology Center Grant P30GM103335 (to J. L.). The authors declare that they have no conflicts of interest with the contents of this article. The content is solely the responsibility of the authors and does not necessarily represent the official views of the National Institutes of Health.

This article contains Figs. S1–S8 and Tables S1–S3.

¹ Present address: Dept. of Physics, Princeton University, Princeton, NJ 08544.

² To whom correspondence should be addressed. Tel.: 301-405-3977; Fax: 301-405-7980; E-mail: bekim@umd.edu.

³ The abbreviations used are: TMD, transmembrane domain; ANOVA, analysis of variance; h, human; m, minimal; BCS, bathocuproinedisulfonic acid; NGM, nematode growth medium; TOF, time of flight; AI, Avoidance Index; qRT, quantitative RT; PAM, peptidyl-glycine α -amidating monooxygenase; ICP-MS, inductively-coupled plasma mass spectrometry.

CHCA-1-mediated copper homeostasis in worms

and *Drosophila melanogaster* Ctr1B transcripts are induced under copper deprivation via the transcription factors Mac1 and MTF-1, respectively (16, 17).

Copper acquisition via CTR1 is vital to maintaining cellular and systemic copper homeostasis. Depleting CTR1 in mice and zebrafish results in lethality at the embryonic stage (18, 19). Conditional knockout of this gene in the mouse intestine leads to severe copper deficiency in peripheral tissues, cardiac hypertrophy, severe viability defects, and accumulation of nonbioavailable copper in the intestine (20). Cardiac-specific *Ctr1* knockout mice exhibit elevated intestinal ATP7A expression and serum copper and decreased hepatic copper storage (21). However, the mechanisms underlying the systemic response to dietary- or tissue-specific copper deficiency remain unelucidated.

We have chosen *Caenorhabditis elegans*, a tractable, multi-tissue organism to explore copper homeostasis and to investigate these unknowns at the systemic level. *C. elegans* has been proven to be amenable to nutrient absorption and distribution studies with zinc, iron, and heme (22–25). Several players in copper trafficking have been delineated in *C. elegans*, including metallothionein, CUC-1, and CUA-1 (26, 27). CUA-1 has been functionally characterized as a key intestinal copper exporter responsible for maintaining systemic copper homeostasis (28). However, mechanisms by which *C. elegans* acquires copper have yet to be characterized. In this study, 10 CTR ortholog genes are identified in *C. elegans*; of these, CHCA-1 is functionally characterized. We show that *chca-1* is transcriptionally regulated by copper in both the intestine and hypodermis and is essential for normal copper level, growth, and reproduction. Furthermore, we found that altered copper balance caused by the loss of CHCA-1 resulted in defects in copper-responsive behavior. Identification of this CTR-like gene in *C. elegans*, which appears to be essential for normal copper balance, illustrates the importance of copper delivery via CHCA-1 for normal metazoan development and behavioral phenotypes.

Results

Copper-responsive transcriptional regulation of CTR1-like genes in *C. elegans*

To identify potential genes for copper acquisition in *C. elegans*, a Basic Local Alignment Search Tool (BLAST) search was performed using the human CTR1 protein sequence as a probe. Unlike many characterized organisms that contain two or three CTR homologs (10, 17, 18, 29), 15 protein orthologs encoded by 10 gene loci are predicted to be potential *C. elegans* CTR genes. The BLAST result scores for the 15 candidate proteins demonstrate that, in general, worm CTR candidates share 30–40% amino acid sequence identity with hCTR1 (Table S1). Worm CTR1 candidate proteins were further analyzed based on the conserved features of CTR proteins, such as number of transmembrane domains and copper-transporting motifs at the N and C termini, and the second predicted TMD. In general, *C. elegans* CTR candidates have a shorter N terminus as compared with human and mouse CTR1 (Fig. S1). Candidate proteins expressed at *F31E8.4*, *Y58A7A.1*, *F58G6.3*, *F58G6.7*, and *F58G6.9* gene loci are enriched with both methi-

onine and histidine at the N terminus. All 15 candidates contain a Met–Xaa₃–Met domain within or close to one of the predicted TMD.

CTR1 abundance is regulated by copper availability. In yeast and mammalian cells, high copper induces CTR1 protein degradation, whereas copper deprivation stabilizes the protein (13, 30, 31). In yeast, such regulation occurs at the transcriptional level. CTR1 expression is induced under copper-depleted conditions by the transcriptional factor Mac1 (2). To test whether worm CTR mRNA abundance can be regulated by altered copper status, qRT-PCR was performed for the 10 candidate genes under optimal, high, and low copper conditions in liquid axenic growth media. To determine the desired range of copper concentration for worm growth, the *C. elegans* Habituation and Reproduction (mCeHR) axenic liquid culture (22) was further modified to contain minimal levels of copper (“low copper” mCeHR). Around 100 synchronized L1 stage worms were grown in axenic culture supplemented with various concentrations of copper chloride (CuCl₂) or bathocuproinedisulfonic acid (BCS, a Cu(I) chelator) for 9 days; the total worm number was counted for each condition on day 9. Supplementation with 10 μM copper was most favorable for worm growth, whereas worms exhibited the defects in development or embryogenesis under both copper-replete and copper-deficient conditions, resulting in significantly decreased total populations (Fig. 1A). Either 10 μM copper, 300 μM copper, or 100 μM BCS was applied to generate normal, strong copper-overload and strong copper-deficiency conditions, respectively, to measure changes in gene expression. Synchronized L1 worms were cultured to the L4 stage, and levels of mRNA of each candidate gene under high- and low-copper conditions were calculated by normalizing to expression levels under the 10 μM copper condition. Under copper-deprived conditions, expression of only *F58G6.3*, *F58G6.7*, and *F58G6.9* was significantly elevated (Fig. 1B). These three genes, together with other candidate genes such as *F01G12.1*, *Y58A7A.1*, and *K12C11.6*, had expression suppressed by 300 μM copper (Fig. 1C).

Importance of CTR1 candidate genes for growth, reproduction, and copper accumulation in worms

Our recent studies have shown that limited availability of dietary copper causes developmental defects in worms and that depletion of the copper exporter CUA-1 in the intestine inhibits copper distribution to peripheral tissues, resulting in reduced growth and brood size (28). To test whether our potential CTR genes were required for worm growth in a copper-dependent manner, L1 stage worms were grown on NGM media plates seeded with OP50 bacteria. Plates were supplemented with either 150 μM CuCl₂, 50 μM BCS, or nothing. Milder copper conditions were used (as compared with the experiments in Fig. 1) to more closely mimic physiologically-relevant conditions of copper abundance and deprivation and to enable observation of intermediate growth phenotypes. Following 3 days of growth, *F58G6.9*- and *F27C1.2*-depleted P₀ animals cultured with 50 μM BCS were found to be stage-delayed, as indicated by time of flight (TOF, worm length quantification), compared with vector-treated animals (Fig. 2, A–D). There were no apparent growth defects observed in worms treated with RNAi

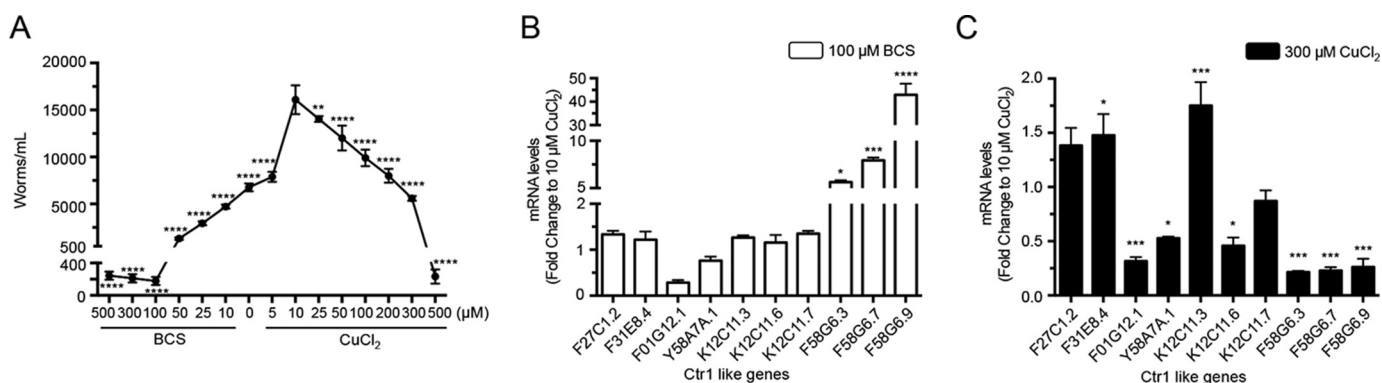


Figure 1. Transcriptional regulation of *C. elegans* CTR1 candidate genes by copper. A, copper-dependent *C. elegans* growth in axenic media. Total worm numbers were calculated for three independent experiments. Asterisks indicate significant difference from optimal 10 μM CuCl₂ condition (one-way ANOVA, Dunnett post hoc test, **, $p < 0.01$; ****, $p < 0.0001$). B and C, qRT-PCR analysis of *C. elegans* CTR candidate genes under copper-limited (B) and high-copper (C) conditions. Worms were synchronized and supplemented with 100 μM BCS, 10 μM CuCl₂, or 300 μM CuCl₂ from the L1 to L4 stage in axenic media. Individual gene expression was normalized first to *pmp-3* and then to its own expression under copper-optimal conditions. Two independent experiments were conducted under each condition. Asterisks indicate significant difference from indicated gene expression levels under optimal conditions. (Two-way ANOVA, Sidak post hoc test, *, $p < 0.05$; **, $p < 0.01$; ****, $p < 0.0001$.) Error bars, mean ± S.E.

against other CTR-like genes under different copper conditions (Fig. 2, A–C) suggesting an important role of the proteins encoded by *F27C1.2* and *F58G6.9* in response to copper deficiency in worms.

To determine the efficiency of knockdown, qRT-PCR was performed to test candidate gene expression levels after RNAi treatment. The mRNA levels of all candidate genes were significantly decreased after worms were fed RNAi bacteria. Although *F01G12.1*, *F31E8.4*, and *K12C11.3* transcripts exhibited a mild reduction (~80–60% of WT expression), silencing of all other CTR candidates was highly effective (less than 30% of WT expression) (Fig. S2).

To further test whether CTR candidates are important for normal copper levels in worms, each gene was individually silenced, and whole-body metal levels were examined by ICP-MS. When providing synchronized L1 (P0) with sufficient copper (10 μM) for two generations, F₁ worms lacking a number of the candidate genes displayed decreased copper accumulation (73–80% of that of vector) (Fig. 2E). To identify the gene most strongly associated with copper accumulation in *C. elegans*, a copper-pulse assay was conducted on each RNAi-treated candidate by pre-culturing worms in copper-limited conditions followed by a 12-h, 50 μM CuCl₂ pulse (Fig. 2F). Following BCS treatment, all worms had extremely low systemic copper concentrations, in a range of 0.03–0.06 μg/g (data not shown). When calculating the level of copper acquired during the copper pulse, *F58G6.3*-, *F58G6.7*-, and *F58G6.9*-depleted worms displayed significant defects in restoration of copper levels. Of these, the most defective were the *F58G6.9* RNAi animals, which only accumulated 40% of the copper measured in vector-treated worms (Fig. 2G). Depleting a number of other candidate genes decreased body copper accumulation under prolonged copper treatment (Fig. 2E). However, these conditions did not significantly impact copper restoration from a copper-deficient state within the time frame assayed, suggesting that these genes, when functioning independently, are not required for effective copper uptake.

Our results narrowed down the CTR-like gene list, leading to *F58G6.9* as the strongest candidate copper importer in worms.

To further explore the role of *F58G6.9* in worm regeneration, we measured brood size in *F58G6.9*-silenced worms under copper-limited conditions. P₀ worms after one generation of *F58G6.9* RNAi under 50 μM BCS supplementation showed substantially smaller brood sizes compared with control animals. Similarly, worms treated with *F58G6.9* RNAi exhibited severe defects in generating embryos when treated with 100 μM BCS (Fig. 2H). Given that the *F58G6.9* gene showed significantly elevated transcript levels under low copper conditions and that it is required for normal growth, reproduction, and copper accumulation in a low-copper environment, we focused on the *F58G6.9* gene as a potential CTR candidate and named it *CTR1* homolog required for copper accumulation-1 (*chca-1*).

CHCA-1 is required for normal copper level and development

We tested functional complementation by worm CHCA-1 in yeast cells defective in the high-affinity copper transporters, Ctr1 and Ctr3, on nonfermentable carbon sources (29). Expression of the CHCA-1 protein with a C-terminal FLAG epitope tag (CHCA-1-2×FLAG) in the heterologous system failed to restore yeast growth (Fig. S3). To test the functional consequence of loss of the endogenous CHCA-1 *in vivo* system, we exploited an established copper-responsive CUA-1–trafficking reporter animal model. Our recent studies have demonstrated that the intestinal CUA-1.1 copper exporter maintains systemic copper homeostasis by altering its subcellular localization (28). It localizes to the basolateral membrane during copper deficiency, and upon copper overabundance, it re-distributes to lysosome-like organelles, called gut-granules, to protect peripheral tissues from copper toxicity. As ICP-MS assays only measure whole-body copper levels, we silenced *chca-1* in transgenic worms expressing CUA-1.1::GFP from the constitutive, intestine-specific *vha-6* promoter (32) (BK015 strain) to evaluate whether the depletion of *chca-1* yields any change in intestinal copper status. Importantly, when given sufficient dietary copper, worms lacking *chca-1* showed CUA-1.1::GFP localized to the intestinal basolateral membrane with significantly decreased distribution to the gut granules when compared with vector-treated animals (Fig. 3A). Individual silencing of all

CHCA-1-mediated copper homeostasis in worms

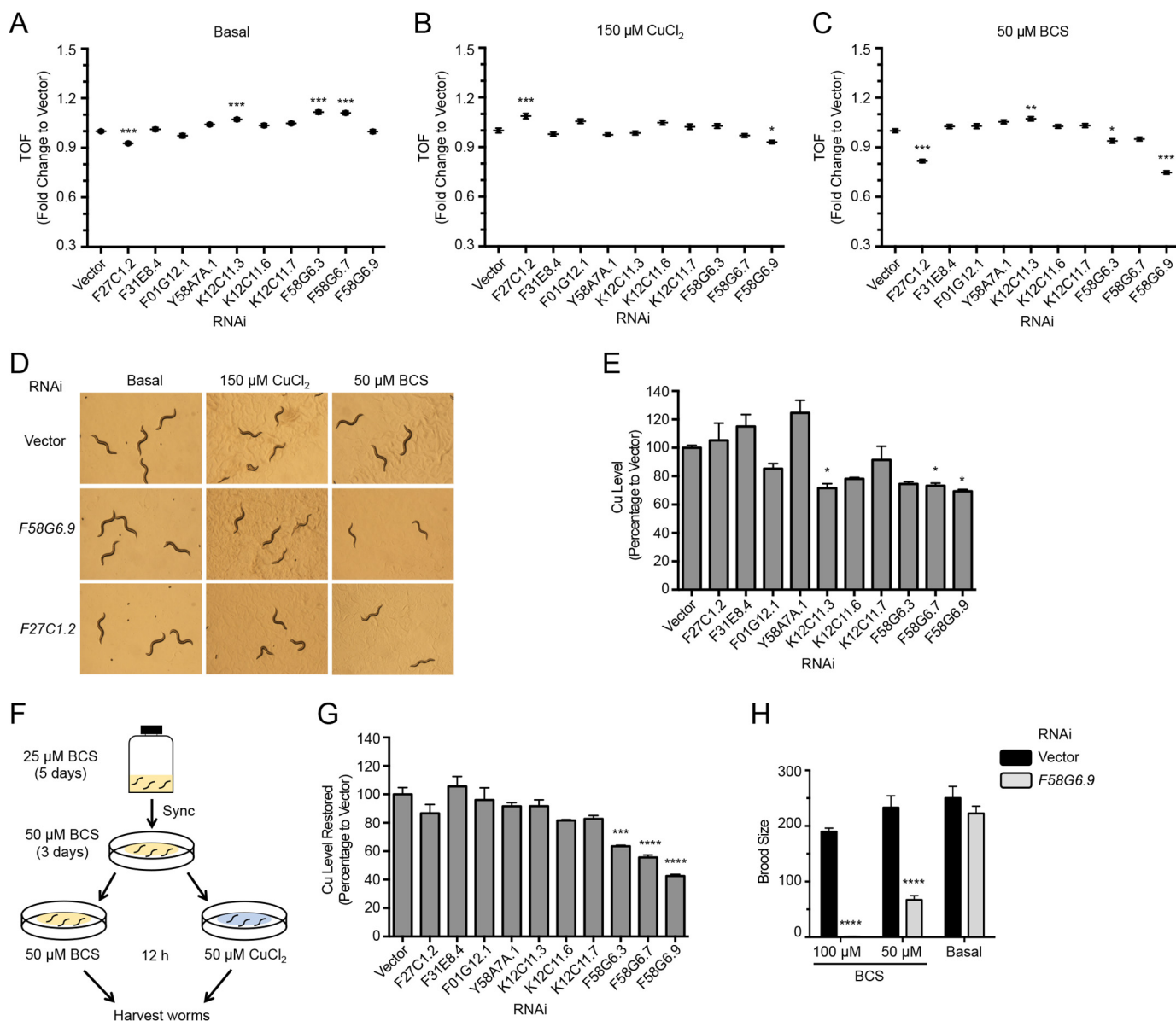


Figure 2. Requirement of *CTR1* candidate genes for growth, reproduction, and copper accumulation in worms. A–C, copper-dependent growth assay under basal (A), high copper (B), and limited copper (C) conditions. Synchronized L1 stage N2 worms were cultured on RNAi plates until the vector-treated worms reached the L4 stage. Worm length (TOF) was quantified using a COPAS BioSort system, and worm length under each RNAi condition was normalized to vector TOF. ~400 individual animals were analyzed under every condition. Values with *asterisk* are significantly different from vector (one-way ANOVA, Dunnett post hoc test, *, $p < 0.05$; **, $p < 0.01$; ***, $p < 0.001$). D, representative images of P₀ worms treated with indicated dsRNA-expressing bacteria. E, copper levels in *C. elegans* were measured by ICP-MS after exposure to 10 μM copper for two generations. Values with *asterisk* are significantly different from vector with three independent trials (one-way ANOVA, Dunnett post hoc test, *, $p < 0.05$). F, schematic presentation of copper-pulse assays. G, restored copper levels under indicated RNAi treatments. Values with *asterisk* are significantly different from vector (one-way ANOVA, Dunnett post hoc test, ***, $p < 0.001$; ****, $p < 0.0001$). H, brood size analysis of *F58G6.9* RNAi animals. Error bars indicate mean \pm S.E. of five independent experiments. Values with *asterisk* are significantly different from vector under the same culture condition (two-way ANOVA, Sidak post hoc test, ****, $p < 0.0001$). Error bars in this figure represent mean \pm S.E.

other *CTR* candidate genes did not change CUA-1.1 localization in the intestine (Fig. S4), suggesting the CHCA-1 is a major player in intestinal copper homeostasis. Our studies have also shown that endogenous CUA-1.1 expression is induced in the hypodermis under dietary copper restriction (28). Upon depleting *chca-1* in transgenic worms expressing CUA-1.1::GFP driven by its own promoter (BK017 strain), CUA-1.1 expression was significantly enhanced in the hypodermis under basal

culture conditions at a comparable level to that of the transgenic strain grown in 25 μM BCS (Fig. 3B). Together, copper-dependent CUA-1.1 distribution and expression in worms lacking *chca-1* were similar to dietary copper-deficient worms, suggesting a role for CHCA-1 in copper acquisition in *C. elegans*.

To further characterize CHCA-1 and to verify the RNAi-based findings, a *chca-1* mutant animal (*chca-1* (*tm6506*) IV)

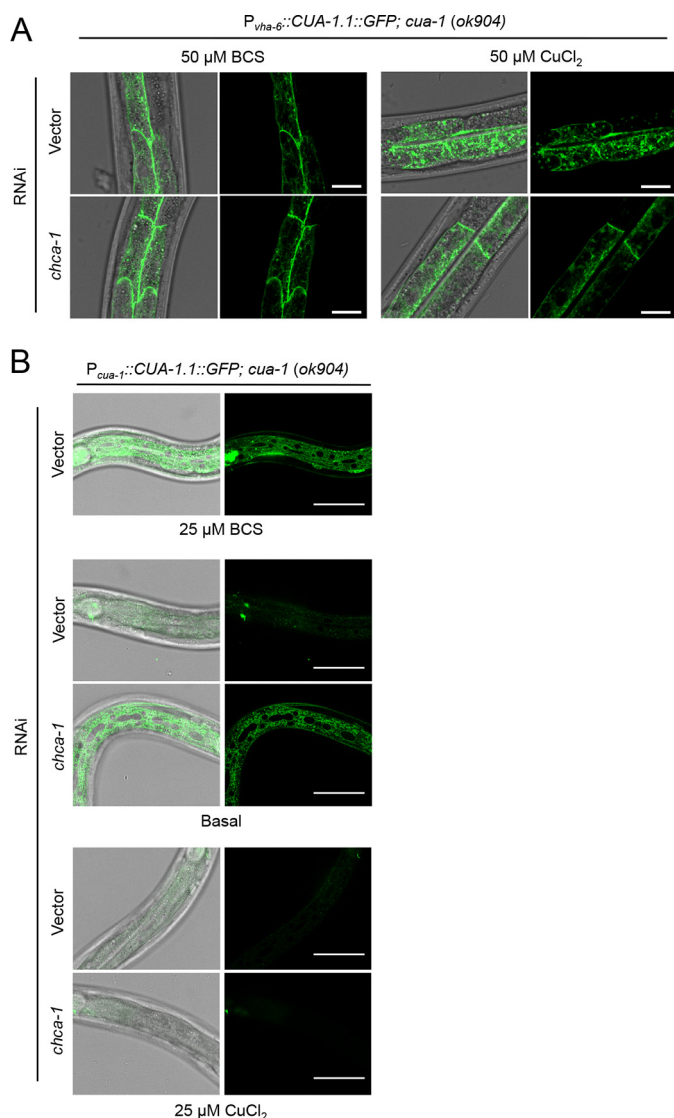


Figure 3. Depletion of *chca-1* gene by RNAi decreases intestinal copper availability in *C. elegans*. A, synchronized L1 stage BK015 transgenic worms ($P_{vha-6}::CUA-1.1::GFP::unc-54\ 3' UTR; cua-1 (ok904)$) were cultured on NGM agar plates seeded with *E. coli* expressing dsRNA against CHCA-1 or vector. CUA-1.1::GFP localization in L4 worms was examined using confocal microscopy. Scale bar, 15 μm . B, *chca-1*-depleted worms display increased endogenous CUA-1.1::GFP expression in the hypodermis. BK017 ($P_{cua-1}::CUA-1.1::GFP::unc-54\ 3' UTR; cua-1 (ok904)$) transgenic animals were maintained on 10 μM CuCl₂ plates prior to synchronization. L1 animals were then re-plated for *chca-1* RNAi. After 60 h of culture, CUA-1.1::GFP expression levels in L4 animals were examined using confocal microscopy. Scale bar, 50 μm .

was obtained from the National Bioresource Project (33). The *tm6506* allele found in this mutant contains a 464-bp deletion that begins in the 5' UTR and spans the second intron of the *F58G6.9* gene; this deletion is predicted to affect the entire N terminus and the first TMD (Fig. 4A and Fig. S5A). Worms homozygous for the *tm6506* allele exhibited defects in growth under basal and copper-replete conditions (10 μM CuCl₂) and showed a severe growth phenotype under BCS treatment within one generation (P₀). However, the growth defects were fully rescued by copper supplementation at 25 μM (Fig. 4, B and C). To test the metal specificity of CHCA-1-dependent growth, 50 μM BCS and several metal sources (CuCl₂, ZnCl₂, FeCl₃, and MnCl₂) were mixed together in the growth media,

and the growth of the *tm6506* mutant strain and its WT out-crossing brood mate (WT) were compared after 3 days of culture. Only copper supplementation rescued the growth defect observed in *chca-1* mutant worms, suggesting a function for this gene in copper-specific regulation (Fig. 4D). Compared with WT animals, *chca-1 (tm6506)* IV worms contained significantly lower copper levels under copper deficiency (ranging from 15 μM BCS up to 10 μM supplemented copper conditions), whereas iron levels were not affected in mutant worms (Fig. S5B); this defect could only be rescued by supplementing the media with 25 μM CuCl₂ (Fig. 4E). Consistent with our RNAi-based results (Fig. 2G), the mutant worms also demonstrated defects in dietary copper acquisition upon copper-pulse (Fig. 4F).

Intestinal CHCA-1 is critical for copper-dependent growth and copper accumulation

To further understand the role of CHCA-1 in copper homeostasis, transgenic worms expressing GFP driven by the endogenous *chca-1* promoter were used to examine tissue-specific expression of this gene. Although the GFP reporter in this strain was barely detectable under copper-replete conditions, it was induced in the intestine and hypodermis upon severe dietary copper deprivation (Fig. 5A). Tissue-specific *chca-1* knock-downs were performed to determine the contribution of CHCA-1 in these two tissues to its systemic role in copper accumulation. This was performed using *rde-1* mutant animals that are RNAi-resistant. In a whole-animal *rde-1* knockout background, knockdown is only effective in a tissue expressing *rde-1* cDNA (34). In this study, the intestine- and hypodermis-specific RNAi-sensitive strains (VP303 and NR222, respectively) were used to deplete *chca-1*, and their growth was compared with whole-body *chca-1* silencing in the N2 strain. Whole-animal RNAi-resistant (WM27) and muscle-specific RNAi-sensitive (WM118) strains served as negative controls. After normalizing the growth of *chca-1* RNAi worms to vector in both P₀ and F₁ generations following RNAi, worms depleted for intestinal CHCA-1 in 100 μM BCS exhibited comparable growth and reproduction defects as to those exposed to whole-body CHCA-1 RNAi depletion. In contrast, worms lacking CHCA-1 only in the hypodermis did not reveal growth defects until the F₁ generation under the same copper-deficient conditions (Fig. 5, B and C). The loss of intestinal *chca-1* was also able to phenocopy the decreased copper levels observed in a whole-animal *chca-1* knock-down (Fig. 5, D and E). These results suggest a dominant function of intestinal CHCA-1 for copper-dependent growth under a copper-limited condition. Meanwhile, CHCA-1 depletion in both the intestine and hypodermis resulted in similar effects on copper accumulation when worms were exposed to 25 μM CuCl₂, a copper-abundance condition (Fig. S6A).

To determine which tissue, when lacking CHCA-1, most significantly contributes to aberrant CUA-1.1 localization in the intestine (Fig. 3A), BK014 transgenic worms ($P_{vha-6}::CUA-1.1::GFP$) were crossed with each of the WM27, VP303, and NR222 strains. Compared with a whole-body knock-down effect (Fig. S6B, panels d and e), loss of CHCA-1 solely in the intestine or hypodermis was not sufficient to increase CUA-1.1::GFP basolateral membrane distribution nor to

CHCA-1-mediated copper homeostasis in worms

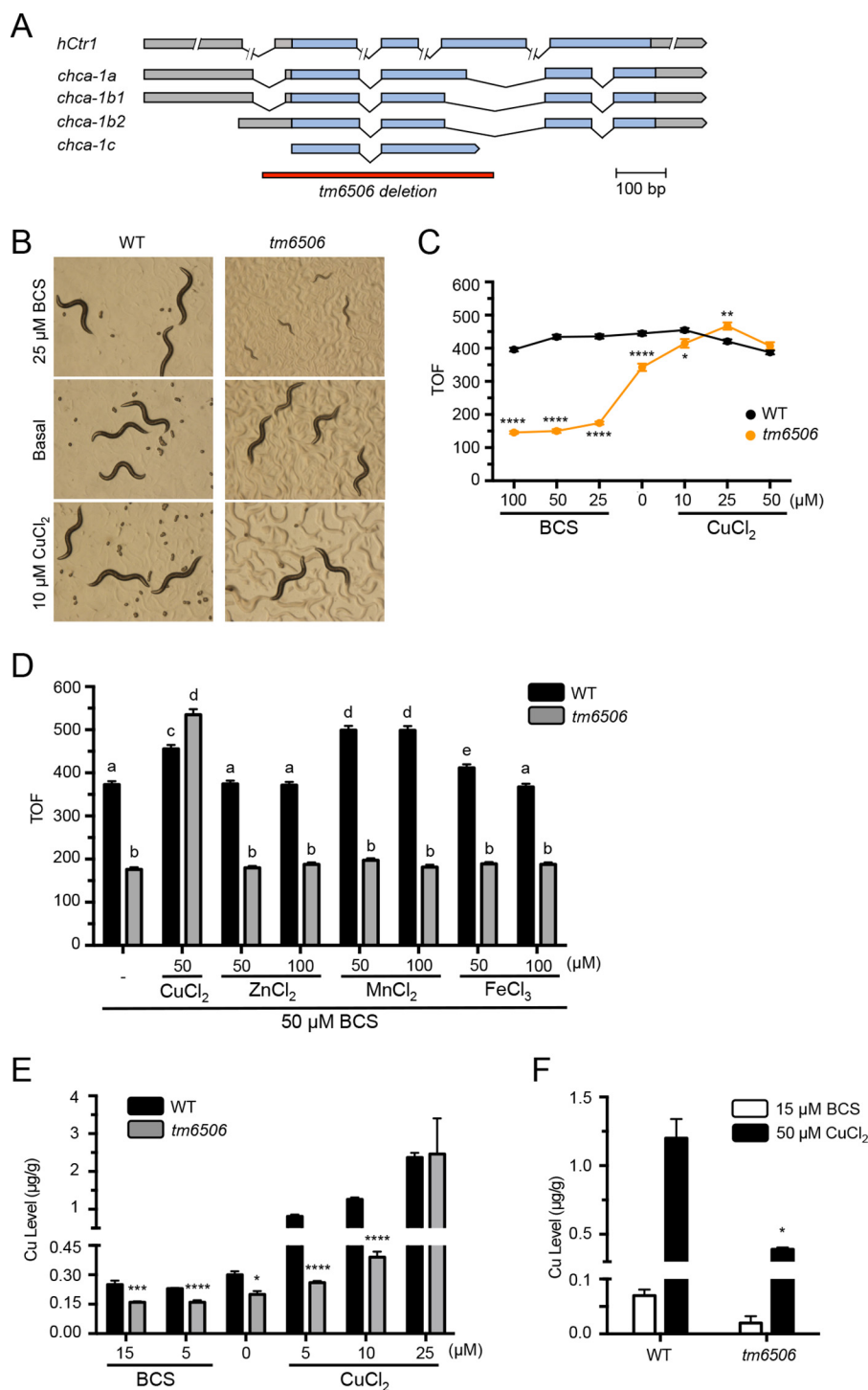


Figure 4. Characterization of the *chca-1* (*tm6506*) IV strain. *A*, schematic of human *CTR1* and *C. elegans chca-1* gene loci, with blue-colored ORFs and gray-colored UTR regions. Note that CHCA-1b1 and CHCA-1b2 isoforms differ at the 5' UTR region but express identical proteins. The deleted region in the *tm6506* allele is indicated by the red bar. Scale bar indicates 100 bp. *B* and *C*, growth of *tm6506* animals under various CuCl_2 - or BCS-supplemented conditions. Worms homozygous for the *tm6506* allele and their outcrossing WT brood mates (WT) were cultured from synchronized L1s for 72 h. *B*, representative images of animals growing under indicated conditions. *C*, worm growth quantification using a COPAS BioSort system. Error bars indicate mean \pm S.E. of around 75 worms. Values with asterisk are significantly different from WT animals under same copper or BCS concentrations (two-way ANOVA, Dunnett post hoc test, *, $p < 0.05$; **, $p < 0.01$; ****, $p < 0.0001$). *D*, WT and *tm6506* mutant worms grown on 50 μM BCS plates or 50 μM BCS plus indicated concentrations of metals. Error bars indicate mean \pm S.E. of around 100 individual animals. Means with different letters are significantly different at $p = 0.05$ (two-way ANOVA, Tukey's post hoc test). *E*, copper levels of *tm6506* and WT animals. Synchronized L1 animals were cultured on indicated concentrations of copper- or BCS-supplemented media for 60 h and then pelleted for ICP-MS. For each condition, three or four samples were analyzed. Values with asterisk are significantly different from those of WT animals (*t* test for each treatment condition, *, $p < 0.05$; ***, $p < 0.001$; ****, $p < 0.0001$). *F*, copper-acquisition capacity of *tm6506* worms. WT or *tm6506* worms pre-treated with 15 μM BCS were washed and separately cultured on fresh 15 μM BCS or 50 μM CuCl_2 NGM plates for 12 h, followed by ICP-MS analysis. Three independent samples were assayed for each condition. Asterisks indicate that copper levels in *tm6506* worms post-pulse are significantly different from those in the WT strain (ANCOVA, Bonferroni post hoc test, $p = 0.016$).

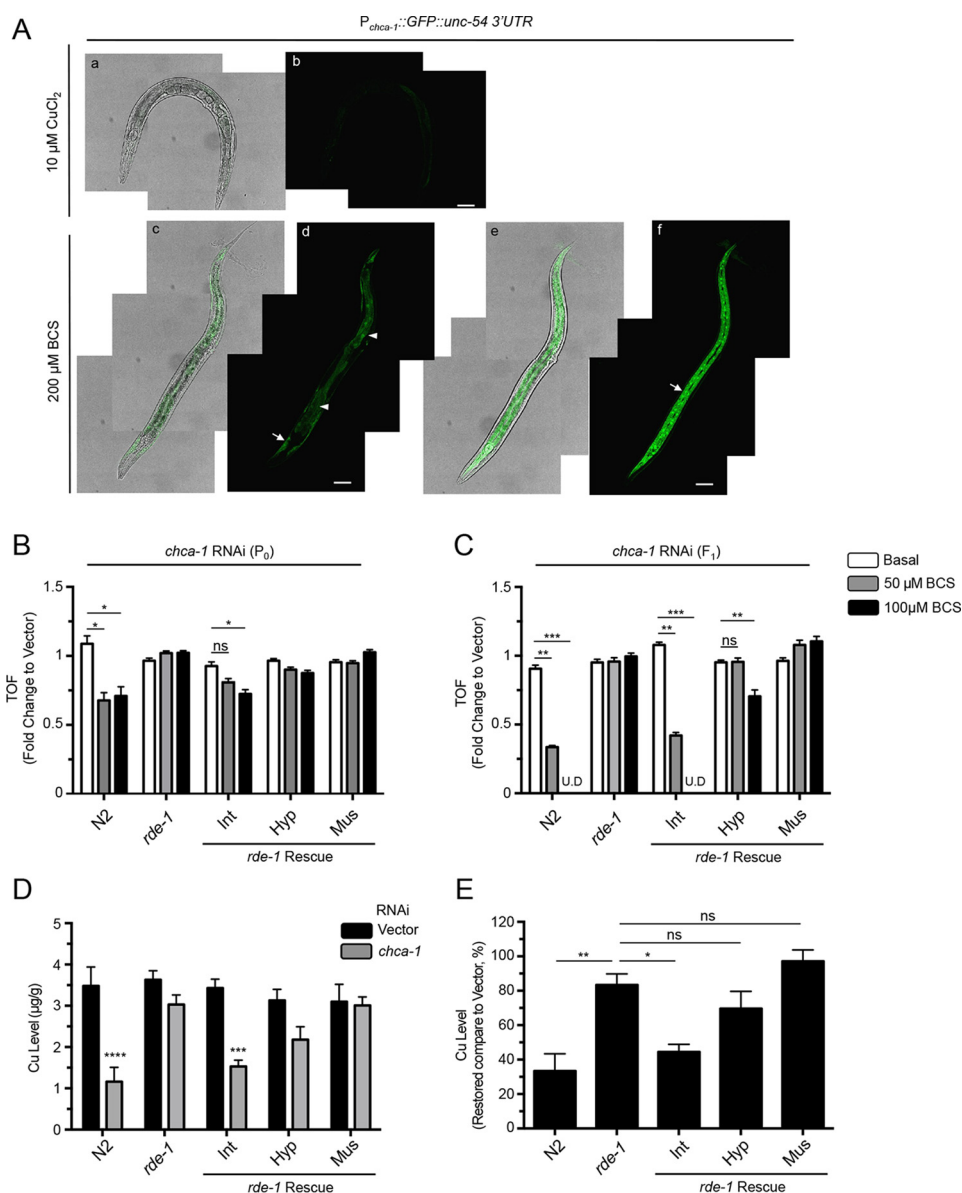


Figure 5. Intestinal CHCA-1 plays an important role in copper-dependent growth and copper accumulation. A, tissue-specific expression of the *chca-1* gene. Transgenic animals expressing GFP driven by the 2.8-kb *chca-1* promoter region were cultured on NGM plates containing $10 \mu\text{M}$ CuCl_2 (panels a and b) or $200 \mu\text{M}$ BCS (panels c–f, same animal, different focus layers). Arrowhead indicates intestine, and arrow indicates hypodermis cells. Panels a, c, and e, bright field; panels b, d, and f, fluorescence. Scale bar, $50 \mu\text{m}$. B and C, copper-dependent growth following *chca-1* gene depletion in specific tissues. N2, RNAi-resistant strains (*rde-1*, WM27) and tissue-specific *rde-1*-expressing strains (VP303, NR222, and WM118) were used to knock down the *chca-1* gene in the indicated tissues (*Int*, intestine; *Hyp*, hypodermis; *Mus*, muscle). Synchronized L1s were cultured to the L4 stage (B, P_0) or re-synchronized and cultured for another generation (C, F_1) on indicated copper-deficient NGM plates prior to quantification. Under each condition, ~ 200 P_0 or F_1 worms' TOF was quantified by a COPAS BioSort. Growth of *chca-1*-depleted worms was normalized to vector for each condition. *chca-1* RNAi in N2 and VP303 strains on $100 \mu\text{M}$ BCS plates exhibited severe defects in P_0 reproduction (U.D., under detection limit). Error bars indicate mean \pm S.E. of ~ 200 individual animals. Values with asterisk are significantly different from the same strain under basal conditions (two-way ANOVA, Dunnett post hoc test, *, $p < 0.05$; **, $p < 0.01$; ***, $p < 0.001$, ns, not significant). D and E, copper accumulation in N2 and tissue-specific *chca-1*-depleted animals. Different strains of worms were pre-cultured on $50 \mu\text{M}$ BCS NGM plates, and then half of the population was separated and treated with copper, as described above in Fig. 2, F and G. D, restored copper levels after normalizing to BCS-cultured samples. Error bars represent mean \pm S.E. of four independent experiments. Values with asterisk are significantly different from vector (two-way ANOVA, Sidak post hoc test, ***, $p < 0.001$; ****, $p < 0.0001$). Copper levels following BCS pre-culture were not significantly different among strains by Two-way ANOVA (data not shown). E, percentage of copper levels restored by *chca-1* RNAi after normalizing to vector animals under the same conditions. Error bars, mean \pm S.E. of four independent experiments. Values with asterisk are significantly different from one another (one-way ANOVA, Dunnett post hoc test, *, $p < 0.05$; **, $p < 0.01$, ns, not significant).

reduce its gut granule expression in the presence of $10 \mu\text{M}$ copper (Fig. S6B, panels n, o, s, and t). These results suggest that both intestinal and hypodermal CHCA-1 play important roles in regulating the copper level in *C. elegans* and raise a possibility that CHCA-1 in the hypodermis could function to compensate copper deficiency in the intestine and/or at the organismal level.

CHCA-1 localizes to intracellular vesicles in the intestine

Given the importance of enterocytes in regulating dietary copper uptake, we generated transgenic worms expressing a CHCA-1::GFP fusion protein driven by the intestine-specific *vha-6* promoter. This fusion protein localizes to vesicles throughout the intestine under basal, copper-deficient, and

CHCA-1-mediated copper homeostasis in worms

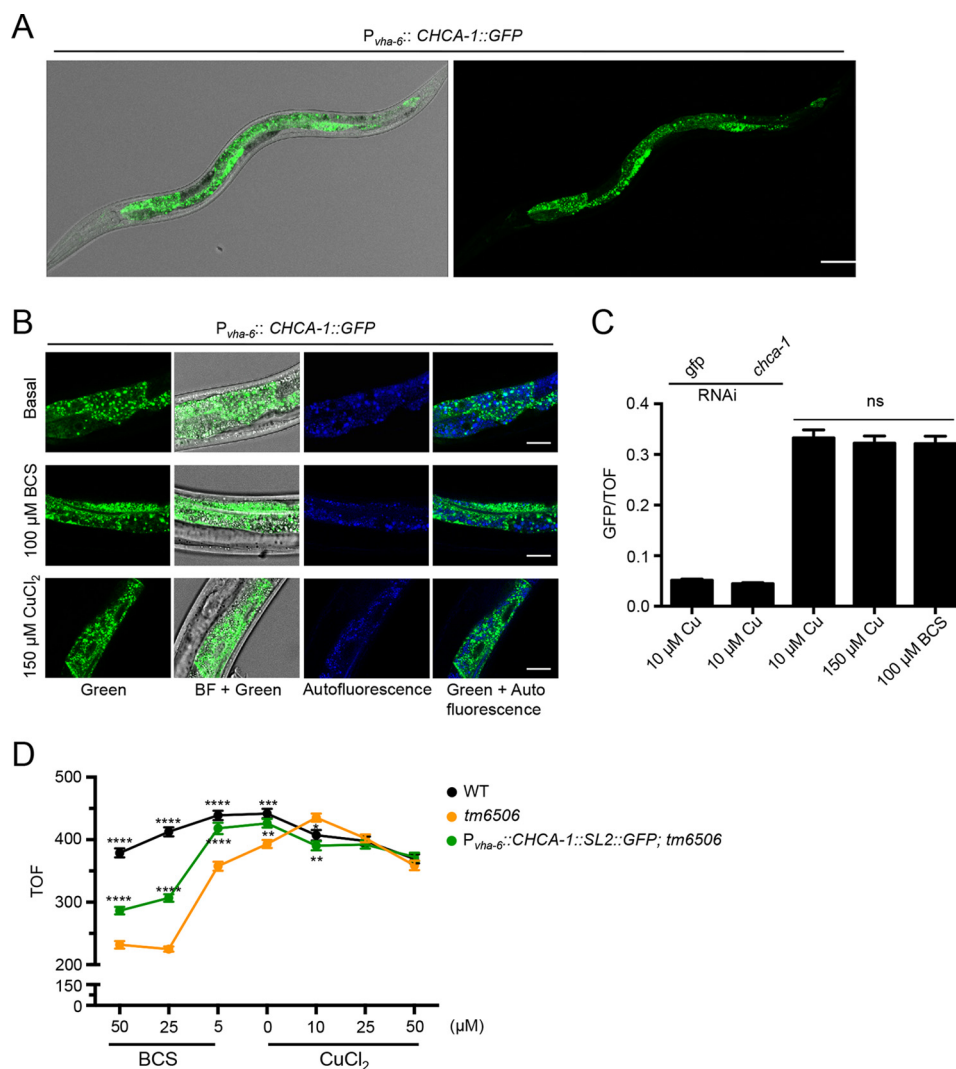


Figure 6. Intestinal expression of CHCA-1::GFP. *A*, intestinal expression of CHCA-1::GFP under basal conditions ($P_{vha-6}::CHCA-1::GFP$, unc-54 3' UTR). Scale bar, 50 μ m. *B*, CHCA-1::GFP expression in the intestine under basal, copper-deficient, and high-copper conditions. A DAPI channel was used to observe intestinal autofluorescence from gut granules. Scale bar, 15 μ m. *C*, CHCA-1::GFP signal intensity was quantified under high, low, or replete copper conditions using a COPAS BioSort system. At least 100 synchronized L4 CHCA-1::GFP-expressing worms were used following 2.5 days of copper or BCS-supplemented cultures in each condition (one-way ANOVA, Dunnett post hoc test, ns, not significant). *D*, intestinal expression of CHCA-1 partially rescued growth of CHCA-1 mutant animals. Transgenic animals expressing CHCA-1::SL2::GFP protein were crossed with *tm6506* animals to generate an intestinal CHCA-1 expression animal in a whole-body *chca-1* mutant background. These transgenic animals, together with their WT brood mates (WT), as well as *tm6506* animals, were quantified by TOF after 60 h of culture from synchronized L1s in the indicated conditions. Error bars indicate mean TOF \pm S.E. of \sim 150 individuals. Values with asterisk are significantly different from *tm6506* worms cultured at the same condition (two-way ANOVA, Tukey's post hoc test, *, $p < 0.05$; **, $p < 0.01$; ***, $p < 0.001$; ****, $p < 0.0001$).

copper-replete conditions (Fig. 6, *A* and *B*). In addition, CHCA-1::GFP expression levels were not altered by copper availability (Fig. 6*C*). Although CUA-1.1 co-localized with a fluorescent copper probe (CF4) in gut granules (28), CHCA-1::GFP did not co-localize with the CF4 or gut granules, the latter of which are autofluorescent (Fig. 6*B*, Fig. S7*A*). To test whether GFP-tagging could lead to CHCA-1 protein mislocalization, a 2 \times FLAG tag, followed by a stop codon and an SL2 splicing leader sequence, was inserted between CHCA-1 and GFP ($P_{vha-6}::CHCA-1-2\times flag::SL2::GFP$). Both GFP and FLAG tags in this study were placed at the C terminus of CHCA-1 to avoid N-terminal truncation observed in mammalian CTR1 (35). The immunofluorescence analysis showed similar vesicle localization of FLAG-tagged CHCA-1 protein (Fig. S7*B*). The function of intestinal CHCA-1 was then tested

by crossing the transgenic worms expressing WT CHCA-1 ($P_{vha-6}::CHCA-1::SL2::GFP$) driven by an intestine-specific promoter onto a *tm6506* mutant background. Transgenic worms expressing WT CHCA-1 in the intestine in the mutant background significantly rescued *tm6506* growth during copper deficiency (Fig. 6*D*). These results suggest a role for vesicular CHCA-1 in mediating copper acquisition in the worm intestine, and that CHCA-1 protein abundance, in contrast with mammalian CTR1, is not regulated by copper status.

CHCA-1 is required for behavioral avoidance of potentially toxic levels of copper

Animals navigate complex natural environments containing both dangerous and valuable items, such as predators and food. *C. elegans* must approach and obtain nutrients while avoiding

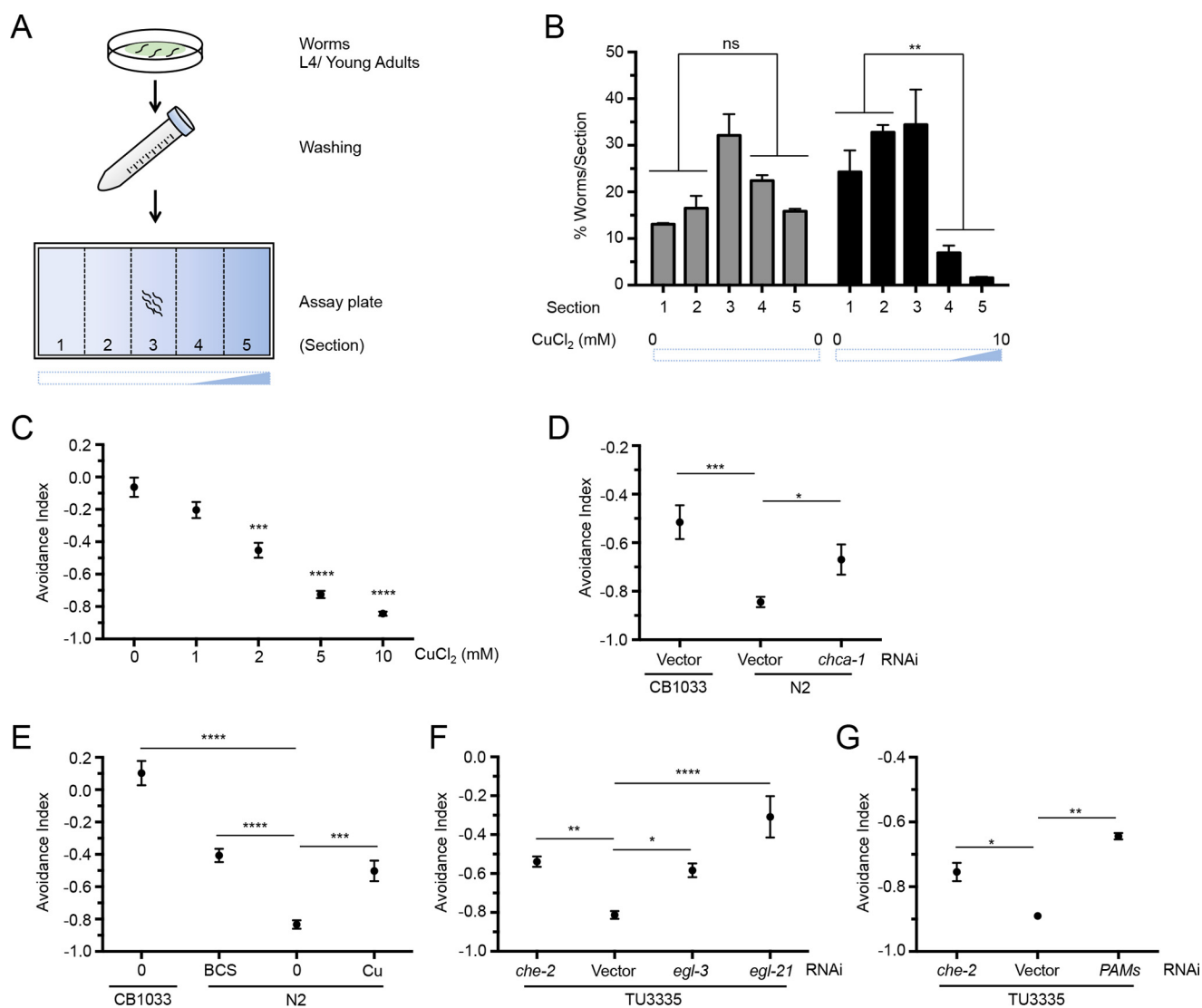


Figure 7. Worms lacking CHCA-1 exhibit reduced copper-sensing behavior. *A*, schematic of copper avoidance assay: copper gradient plates were made by adding a given concentration of CuCl_2 to one side of a rectangular plate. Non-copper-containing plates were used as controls. At least 150 animals were used on each plate with a total of three independent experiments. *B*, representative results of N2 worm distribution on a non-copper plate (left) or 10 mM copper gradient plate (right). Error bars, mean \pm S.E. of two independent experiments. Asterisk indicates the percentage of animals in the low-copper area (sections 1 and 2) is significantly different from the percentage in the high-copper area (sections 4 and 5) (two-way ANOVA, Sidak post hoc test, **, $p < 0.01$, ns, not significant). *C*, N2 worm avoidance index on copper gradient plates with varied concentrations of copper. Error bars indicate mean \pm S.E. of three independent experiments. Asterisk values are significantly different from the avoidance index on non-copper plates (one-way ANOVA, Dunnett post hoc test, ***, $p < 0.001$; ****, $p < 0.0001$). *D*, avoidance index of CB1033 (*che-2* (*e1033*) X) and N2 vector worms or *chca-1* RNAi worms on 8 mM copper gradient plates. Three independent experiments for CB1033 and six independent experiments for N2 were analyzed (one-way ANOVA, Dunnett post hoc test, *, $p < 0.05$; **, $p < 0.01$; ***, $p < 0.001$; ****, $p < 0.0001$). *E*, worms were pre-cultured with 100 μM CuCl_2 or 100 μM BCS for one generation and assayed on 8 mM copper gradient plates. (One-way ANOVA, Dunnett post hoc test, ***, $p < 0.001$; ****, $p < 0.0001$.) *F*, avoidance index of RNAi-hypersensitive worms (TU3335) lacking the *egl-3* or *egl-21* gene on 10 mM copper gradient plates. Error bars indicate mean \pm S.E. of eight independent experiments under each condition. Values with asterisk are significantly different from each other (one-way ANOVA, Dunnett's post hoc test, *, $p < 0.05$; **, $p < 0.01$; ****, $p < 0.0001$). *G*, PAM genes (*pgal-1*, *pghm-1*, and *pamn-1*) were co-depleted by RNAi for two consecutive generations in TU3335 strain, followed by the avoidance assay on 10 mM copper gradient plates. Error bars indicate mean \pm S.E. of two independent experiments. Values with asterisk are significantly different (one-way ANOVA, Dunnett post hoc test, *, $p < 0.05$; **, $p < 0.01$).

various threats, which include toxic levels of copper. Worms detect threats via primary sensory neurons that then propagate such information through an interneuron network to ultimately reach pre-motor command interneurons that direct controlled locomotion. Thus far, several ciliated sensory neurons (ASH, ASE, ADL, ASI, and ADF) are known to correlate with copper sensing and/or avoidance behavior (36, 37). We studied whether altered copper status in worm affects its copper avoidance behavior. To quantify levels of avoidance, assays were performed on rectangular plates containing a

gradient of CuCl_2 , from no copper supplementation on one end to toxic copper levels on the other end. After production, assay plates were kept in a cold chamber for a defined period of time to allow for copper diffusion and concentration gradient formation and then were marked in sections (Fig. 7A). With copper supplementation, plates generated with the method described above contain a sharp copper gradient ranging from section 3 to section 5, as measured by ICP-MS performed on agar samples from the gradient plates (Fig. S8A).

CHCA-1-mediated copper homeostasis in worms

Stage-synchronized L4 young adult worms were seeded in the middle of the bacteria-free copper gradient plates, and worm distribution after 2.5 h was visualized. During quantification, each plate was evenly divided into five sections (with section 5 representing the highest copper level area), and a formula was used to calculate the avoidance index (AI) as described under “Experimental procedures.”

We observed that WT N2 worms on the copper gradient plates (10 mM copper) had a strong tendency to avoid high copper-containing areas (Fig. 7B) as compared with normal distribution of worms on non-copper plates. Changing the maximum concentrations found in the copper gradient from 1 to 10 mM led to N2 worms exhibiting enhanced avoidance (Fig. 7C). For further assays, 8 or 10 mM copper gradients were chosen to achieve clear resolution under tested conditions. On 8 mM copper gradient plates, *che-2* mutant animals (CB1033), of which sensory cilia formations are defective (38), lacked copper avoidance behavior compared with N2 worms, supporting the importance of the chemosensory axis in copper sensing. Meanwhile, *chca-1*(RNAi) worms demonstrated decreased levels of avoidance (Fig. 7D), suggesting that CHCA-1 is required for a role in sensing and avoiding toxic copper concentrations. To test whether altered systemic copper levels in *chca-1*(RNAi) worms result in changes to avoidance behaviors, both copper-deprived and copper-overloaded worms were generated by preculturing N2 worms in 100 μ M BCS or copper conditions and, along with N2 worms cultured in basal media, were placed on copper gradient and non-copper-plates. The copper-deficient worms exhibited less avoidance compared with nonprecultured worms, which recapitulated the behavior of *chca-1*(RNAi) worms. However, interestingly, copper-overloaded worms also revealed less avoidance of toxic copper (Fig. 7E). These results suggest that in *C. elegans* the copper-sensing behavior is correlated with abnormal copper levels, although the precise mechanisms that determine this behavior remain elusive.

Copper is known to be crucial for the neuropeptide maturation process through the copper-dependent peptidyl-glycine α -amidating monooxygenase (PAM) (39). To test whether neuropeptides are important for copper-sensing behavior in worms, using RNAi-hypersensitive strains that allow mRNA silencing in neurons (40), the proprotein convertase *egl-3* and the carboxyl peptidase *egl-21* were silenced individually (41, 42), and a significantly decreased avoidance behavior was observed (Fig. 7F). Furthermore, depletion of all predicted PAM orthologs in *C. elegans* (*pgal-1*, *pghm-1*, and *pamn-1*) caused reduced copper avoidance (Fig. 7G). Gene-silencing efficiency was tested by qRT-PCR performed in parallel to the RNAi experiments. After RNAi treatment, mRNA levels of *che-2*, *egl-3*, *egl-21* and PAMs were decreased (Fig. S8B). Taken together, our results suggest that copper-sensing and/or corresponding behavior of *C. elegans* is associated with the copper-dependent neuropeptide maturation in neurons that requires CHCA-1 activity and balanced body copper levels.

Discussion

Copper acquisition via CTR family proteins is critical for survival during fluctuations in environmental copper levels. Our

studies reveal that, similar to yeast, fish, and mammals, worms lacking CHCA-1 have lower systemic copper levels and exhibit profound growth and reproductive defects under low copper availability. Our results with worm CTR candidates also suggest that the pathway for copper trafficking to the secretory pathway via the CTR1-ATOX1-ATP7A/B axis in mammals is conserved in worms. *C. elegans* can thus be exploited as a facile whole-live animal system to isolate novel components regulating copper homeostasis, as well as providing additional insight into known components.

For example, the fact that *C. elegans* CHCA-1 is predicted to lack a third TMD, as well as lacking a C-terminal cysteine or histidine residue, calls into question the minimal structural requirements for a high-affinity copper transporter. Additionally, although yeast copper metabolism components are regulated transcriptionally, and mammalian copper metabolism components are generally regulated at the post-translational level, worms exhibit characteristics of both. CTR homolog genes, such as *F58G6.3* and *F58G6.7*, are transcriptionally regulated by copper. The worm ATP7A/B homolog, CUA-1, is regulated both transcriptionally and post-translationally (28). *C. elegans* may thus shed light on the evolutionary history of copper metabolism regulation. Importantly, we show differing contributions of CHCA-1 to systemic copper metabolism depending on whether it is expressed in the intestine or in the hypodermis. Thus, *C. elegans* also provides insight into coordination of copper homeostasis in multiple tissue organisms.

Uncovering 10 CTR candidate genes in *C. elegans* was unexpected, as other model organisms contain fewer CTR homologs. Individually silencing these candidate genes did not severely affect worm growth or copper accumulation under basal or copper-replete conditions (Fig. 2, A and E). Although non-CTR ortholog metal importers could contribute to dietary copper uptake in *C. elegans*, it is also likely that several CTR genes function redundantly or that CTR proteins form higher-order heteromultimers, which serve as fully active copper transporters (43). Considering that CHCA-1 is dominantly enriched only in the intestine and hypodermis, it is possible that other CTR proteins in *C. elegans* are expressed in different tissues and/or are required under different copper conditions or during specific developmental stages.

Although studies demonstrate that mammalian CTR1 constitutively cycles from endosomal compartments to the plasma membrane in many cultured cell lines (30), and endogenous mouse CTR1 is localized to both the apical membrane and intracellular compartments of intestinal epithelial cells in mouse models (20), our data demonstrate that CHCA-1 localizes mainly to intracellular vesicles with minimal localization to the apical membrane. Reports in *C. elegans* have identified lysosome-like compartments known as gut granules in the intestine that could serve as a buffering subcellular organelle by transporting metals in the compartment under copper or zinc overload conditions (28, 44). It is plausible that copper stored in gut granules could be recycled by CHCA-1 upon a copper-starvation stock. However, CHCA-1::GFP was not found to co-localize with gut granules. These results suggest that CHCA-1 may function to transport copper across from the lumen of an as-yet-undefined intracellular compartment, whereas other

copper importers drive copper transport across the plasma membrane. Further studies will be necessary to ascertain whether CHCA-1 is important for the mobilization of copper from endosomes.

In addition to the intestine, a significant induction of *chca-1* expression in the hypodermis is also observed under copper deprivation. Similarly, *cua-1* abundance also increases in the hypodermis during copper deficiency, for which regulation may also occur at the transcriptional level (28). The hypodermis is known to play a role in iron (45) and heme homeostasis in worms (46); as such, these findings strengthen its potential role in copper homeostasis. It is plausible that hypodermal CHCA-1 acquires copper to incorporate into the secretory pathway through CUA-1 activity. Alternatively, CHCA-1 in the endosomes together with CUA-1 in the plasma membrane may function to recycle stored copper in the hypodermis to peripheral tissues in response to systemic copper deficiency, as the worm hypodermis is known to store other nutrients (47).

Dwelling in the soil, *C. elegans* encounters a complicated and mercurial environment requiring flexible responses to pathogen exposure, gas composition, and temperature transitions, as well as undesirable nutrient concentrations. Behavioral studies in worms under varying environmental stimuli have led to important discoveries, establishing the sensing and signaling axis toward CO₂/O₂ and temperature (48–52). High concentrations of copper are used as a chemical repellent, and several copper chemosensory neurons have been identified (36, 37). In this study, CHCA-1 was shown to be required for sensing and avoiding copper, possibly via downstream effects of systemic copper scarcity, as worms lacking CHCA-1 or with limited dietary copper sources both revealed significantly decreased avoidance to toxic levels of copper. Further experiments suggest that a neuropeptide maturation process, which is copper-dependent in many organisms, is involved in worm copper sensing and avoiding (Fig. 7, F and G). Copper-deficient worms may have an increased capacity to uptake copper and to be resistant to toxic copper levels, resulting in decreased avoidance in the time frame of our assays. Alternatively, this altered behavior may be due to defects in the biogenesis of neuropeptides required for copper sensing or altered signal transmission to downstream interneurons or motor neurons.

An unanticipated observation from our studies was that dietary copper-overload worms also showed reduced avoidance of toxic copper. It is reported that acute copper exposure induces ASH neuron activity, but repeated copper stimulation leads to the reduction in the avoidance response and in ASH neuronal activity. This may result in changes to receptor activity and any downstream signaling pathways (53). Another explanation could be the failure of sensing caused by copper toxicity during pre-culture in high copper conditions (54). Is there a copper-specific receptor on the neuronal cell surface that elicits subsequent behavioral responses? Could there be a copper-sensing olfactory receptor? Whereas the vertebrate olfactory system has a single receptor gene expressed in each sensory neuron (55), worms have limited numbers of chemosensory neurons, with multiple receptors expressed in one sensory neuron. There are ~1300 receptor genes found based on phylogenetic analysis. Although electrical and hormonal signals are com-

monly used for neuronal signaling, neuropeptides, many of which are thought to be copper-dependent, function as crucial signaling regulators as well (56, 57). Identification of the essential component in the signaling events will provide leads for future studies seeking to understand copper-responsive decision making and behavior in *C. elegans*.

Experimental procedures

Worm strains and culture

C. elegans were cultured at 20 °C on NGM plates seeded with *Escherichia coli* OP50 for general maintenance or with *E. coli* HT115 dsRNA-expressing bacteria for RNAi experiments (58). Bristol N2 was used as the WT *C. elegans* strain. Mutant and transgenic strains were outcrossed with N2 to obtain WT backgrounds, and a WT brood mate animal was used following crossing in mutant and transgenic animal growth/avoidance assays. Some strains were provided by the CGC, which is funded by National Institutes of Health Office of Research Infrastructure Programs (P40 OD010440). The *chca-1* (*tm6506*) IV strain was obtained from the National Bioresource Project (33) and outcrossed with N2 six times prior to use to establish heritability; *CB1033* (*che-2* (*e1033*) X) was obtained from CGC and outcrossed six times before use for the same purpose. A list of transgenic worms used in this study can be found in Table S2. Transgenic animals in a *chca-1* (*tm6506*) mutant background, as well as multiple transgene-presenting strains, were generated with standard mating methods; genotypes were confirmed by PCR and/or DNA sequencing. The *chca-1* (*tm6506*) genotyping primers were 5'-GTATCTAGTCCGATAAGAAG-3' and 5'-TTGAAGCAAAAACAAAGTGC-3'.

Yeast strain and spotting assay

The MPY17 *S. cerevisiae* strains used in this study contained an *scCTR1* and *scCTR3* double deletion (10). Genes were tagged at the C termini with a 2×FLAG sequence and inserted into a pYES3 vector (59). Plasmids containing either FLAG gene insertions or FLAG tag only were transformed into *CTR1ΔCTR3Δ* yeast. Yeast strains were maintained in a synthetic complete medium (SC) lacking uracil for plasmid selection. Spotting assays were conducted on YPD (1.5% agar, 2% bacto-peptone, 2% glucose, 1% yeast extract) and YPEG (1.5% agar, 2% bacto-peptone, 3% glycerol, 2% ethanol, 1% yeast extract) media. Cells with an A₆₀₀ of 0.2 (7 μl) were spotted onto growth media in a series of 10-fold dilutions. Expression was induced by adding 0.4% galactose into the media. Pictures were taken following incubation at 30 °C for 5 days following spotting.

RNAi

HT115 (DE3) bacterial strains containing plasmids expressing dsRNA against *F27C1.2*, *F31E8.4*, *Y58A7A.1*, *F58G6.7*, *F58G6.9*, *K12C11.6*, and *K12C11.7* genes were obtained from the Ahringer and ORFeome feeding libraries (60, 61). The empty vector L4440 was used as a control. Portions of *F01G12.1*, *K12C11.3*, and *F58G6.3* DNA constructs were cloned into the L4440 vector and transformed into HT115 bacteria. Each construct was sequenced using the primer 5'-AGC-

CHCA-1-mediated copper homeostasis in worms

GAGTCAGTGAGCGAG-3' and evaluated by the E-RNAi online tool to determine the RNAi target. NGM growth media with 12 $\mu\text{g/ml}$ tetracycline, 50 $\mu\text{g/ml}$ carbenicillin, and 2 mM isopropyl 1-thio- β -D-galactopyranoside were used for RNAi experiments.

BLAST and topology prediction

The human CTR1 protein sequence was used as a query sequence in a search using PSI-BLAST. Nonredundant (nr) protein sequences were chosen for the database, and results were filtered to include only hits on the *C. elegans* (taxid:6239) genome. Candidates had an E-value cutoff of less than 10^{-3} . TMD of various organisms' CTR homologs were predicted by TMHMM 1.0. Clustal Omega was used to generate sequence alignment.

Axenic media growth

The axenic liquid media used in this study ("low copper" mCeHR) is modified from the mCeHR media described previously (22) by removing extra copper supplementation in the salt solution. 20 μM hemin is added for every culture condition. N2 worms grown in "low copper" mCeHR media were synchronized and hatched overnight in M9 buffer. Approximately 100 L1 stage worms were seeded into a 10-ml liquid media-containing flask with indicated CuCl_2 or BCS concentrations. Flasks were incubated on a rotating platform at 20 °C for 9 days. On day 9, animals were collected; samples were centrifuged (800 \times g, 1 min) to collect worm pellets and then washed twice with M9 buffer. To count the number of worms, the tube was vortexed to mix, a prescribed amount of sample was drawn up and placed on a slide, and worm counts were calculated. Each condition was tested and counted in triplicate.

qRT-PCR

For assays conducted in axenic media, N2 worms were maintained in 10 μM CuCl_2 low copper mCeHR and then synchronized and split into flasks containing 10 μM CuCl_2 (optimal), 300 μM CuCl_2 (high copper), or 100 μM BCS (low copper) media. Worms were grown in each condition until the population reached the mid-L4 stage. Worms were collected after washing twice with M9 buffer and resuspended in 1 ml of TRIzol (Invitrogen) and then lysed in Lysing Matrix Tubes (MP Biomedicals) by FastPrep-24 (MP Biomedicals) homogenizer. Total RNA was isolated using the NucleoSpin RNA kit (Macherey-Nagel), and 1 μg of RNA was used for cDNA synthesis (SuperScript III First Strand synthesis kit, Invitrogen). Real-time PCR was performed with SYBR Green Taq 2 \times Mix (Bio-Rad) with three biological replicates and two technical replicates. Fold-change values were calculated using the $2^{(-\Delta\Delta C_t)}$ method, with all values normalized to *pmp-3* (Fig. 1, B and C) or *gpd-2* (Figs. S2 and S8B) expression. Primers are listed in Table S3.

Quantification of copper-dependent worm growth, length, brood size, and copper levels

Assays were performed as follows, unless specified in figure legends. For worm growth assays and length quantification, stage-synchronized L1 worms (P_0) were grown on RNAi-ex-

pressing bacteria until vector-fed control worms reached the L4 stage. P_0 worms were washed off the culture media with M9 buffer, and 100 μl of worms in M9 buffer were transferred into a 96-well culture dish. Animals' body length (TOF), density (extinction), and fluorescence intensity were quantified using a COPAS Biosort system FP-250 (Union Biometrica). To perform these assays on F_1 worms, 20 P_0 worms were transferred to fresh plates at the L4 stage and allowed to lay eggs for 12 h after reaching the gravid adult stage. P_0 worms were removed from the plate, and F_1 progeny were analyzed as above upon reaching the L4 stage.

For brood size analysis, synchronized L1 worms were cultured on dsRNA-expressing bacteria for 50 h until reaching gravid adult stage. Individual worms were then transferred onto fresh plates to allow egg laying. After 3 consecutive days of egg laying, the brood size, including both hatched and unhatched embryos, was counted.

For copper-pulse experiments, a mixed stage population was cultured on BCS-supplemented NGM plates for 5 days prior to synchronization. BCS-treated worms were then bleached to generate synchronized L1 animals that were then cultured on BCS plates for 48 h, washed off, and split evenly onto BCS- and copper-supplemented plates for 12 h prior to worm pelleting. Restored copper levels for each experimental condition were normalized to BCS-treated samples. See below for ICP-MS measurements.

ICP-MS

Metal contents of worms were measured using ICP-MS as described previously (20). Values were normalized to wet weight of worms. For sample preparation, synchronized L1 worms were grown on NGM plates seeded with OP50 or HT115 RNAi bacteria and supplemented with the indicated amounts of copper or BCS until worms reached L4 stage. Worm pellets were collected and washed extensively with M9 buffer, transferred to acid-washed tubes, and frozen at -80 °C. At least three independent biological replicates were analyzed.

Generation of transgenic worms

Transgene-expressing plasmids were generated using a Multisite Gateway Three-Fragment Vector Construction kit (Invitrogen). Promoter, ORF, and UTR regions were amplified separately and recombined into the plasmid. The *unc-54* 3' UTR region is used in all constructs in this study. Together with the *unc-119* rescue plasmid, the transgene-expressing plasmid was then introduced into *unc-119* (*ed3*) III worms using a PDS-1000 particle delivery system (Bio-Rad) bombardment system. To generate worm strains expressing multiple transgenes, one worm strain expressing a single transgene was crossed with another transgenic worm using methods previously described (62).

Staining with the copper probe CF4

Stage-synchronized L4 worms expressing CHCA-1::GFP in the intestine were used for the CF4 assay. Worms were washed three times with M9 buffer, and around 400 worms were suspended in 100 μl of M9 buffer. CF4 copper probe (28) was then added to the buffer at a concentration of 25 μM . Worms were

stained in the dark at room temperature for 2 h and then transferred onto normal NGM plates outside the bacterial lawn. These plates were kept in the dark for 2 h, and then the worms were collected and washed three times with M9 buffer and imaged via confocal microscopy.

Copper-responsive behavior assay

The copper-avoidance assay in this study utilized rectangular copper gradient plates. To make copper gradient media, 4-well rectangular plates were tilted on their lids, and 2 ml of copper-containing media (with indicated concentrations of CuCl₂ in 1.7% agar, 3 mg/ml NaCl, 5 μg/ml cholesterol, and 2.5 mg/ml bacto-peptone) was added to one-third of the plate length. Upon solidification, plates were brought flat, and 10 ml of NGM agar was added on top. For control experiments with non-copper-containing plates, plates received 12 ml of NGM agar alone. After upper layer solidification, plates were kept at 4 °C for 16 h to allow copper diffusion prior to conducting the assay. Five sections were drawn on the bottom of the plates (indicating low to high copper) for future quantification of worms per section as delineated by approximate concentration. Synchronized L4 worms were washed three times with M9 solution to remove bacteria, and 40 μl of worm-M9 solution was pipetted in the middle section of the plate (section three). Following a 2.5-h drying period, images of the plates were captured by camera, and animals in each section were counted using ImageJ software. Each assay included at least 150 animals, and at least three independent experiments were performed for each condition. Avoidance behavior of the high copper regions (sections four and five) were denoted by an AI derived from Equation 1, avoidance index (AI)

$$= \frac{\text{percentage of worms in section } ((4 + 5) - (1 + 2))}{\text{percentage of worms in section } ((4 + 5) + (1 + 2))} \quad (\text{Eq. 1})$$

Worms in section three were not calculated, as not all worms translocated to different sections in the given time frame.

Immunofluorescence and Western blotting

The antibodies applied in the worm immunofluorescence assays are rabbit anti-FLAG (Rockland) at 1:300 and Alexa594 goat anti-rabbit IgG (ThermoFisher Scientific) at 1:300. For each condition, 75 μg of protein was loaded into gels. Transgenic animals expressing CHCA-1-2×FLAG::SL2::GFP in the intestine were stage-synchronized, and L4 worms were fixed and stained with antibody as described previously (63). Worms applied with secondary antibody only served as negative controls. For the yeast Western blottings, rabbit anti-FLAG (Rockland) at 1:2000 and mouse anti-PGK1 (Molecular Probes) at 1:1000 were applied as primary antibodies.

Statistical analysis

Statistical significance was calculated by one-way ANOVA, two-way ANOVA, or a *t* test with Prism GraphPad version 6 (GraphPad, San Diego). Analysis of covariance was performed using SPSS Statistics version 23 (IBM). Data values were presented as mean ± S.E. Asterisks indicate significance at *p* values <0.05.

Author contributions—S. Y. and B.-E. K. conceptualization; S. Y., A. K. S., A. R., J. L., and B.-E. K. data curation; S. Y., A. K. S., A. R., J. L., and B.-E. K. formal analysis; S. Y., A. K. S., A. R., and J. L. validation; S. Y., A. K. S., A. R., J. L., and B.-E. K. investigation; S. Y. visualization; S. Y., A. K. S., A. R., and J. L. methodology; S. Y. writing-original draft; S. Y. and B.-E. K. writing-review and editing; B.-E. K. supervision; B.-E. K. funding acquisition; B.-E. K. project administration.

Acknowledgments—We thank members of the Kim laboratory for helpful suggestions, technical assistance, and critical reading of this manuscript. We thank members of Dr. Iqbal Hamza's laboratory (University of Maryland, College Park) for technical assistance and expertise in *C. elegans* genetics and cell biology as well as for discussions regarding the work, and Dr. Tamara Korolnek for critical reading of this manuscript. The COPAS Biosort instrument was purchased from funds supported by National Institutes of Health Grant DK074797 (to I. H.).

References

- Kim, B. E., Nevitt, T., and Thiele, D. J. (2008) Mechanisms for copper acquisition, distribution and regulation. *Nat. Chem. Biol.* **4**, 176–185 [CrossRef Medline](#)
- Nevitt, T., Ohrvik, H., Thiele, D. J. (2012) Charting the travels of copper in eukaryotes from yeast to mammals. *Biochim. Biophys. Acta* **1823**, 1580–1593 [CrossRef Medline](#)
- Gaetke, L. M., Chow-Johnson, H. S., and Chow, C. K. (2014) Copper: toxicological relevance and mechanisms. *Arch. Toxicol.* **88**, 1929–1938 [CrossRef Medline](#)
- Lutsenko, S., Barnes, N. L., Bartee, M. Y., and Dmitriev, O. Y. (2007) Function and regulation of human copper-transporting ATPases. *Physiol. Rev.* **87**, 1011–1046 [CrossRef Medline](#)
- Ohrvik, H., and Thiele, D. J. (2014) How copper traverses cellular membranes through the mammalian copper transporter 1, Ctr1. *Ann. N.Y. Acad. Sci.* **1314**, 32–41 [CrossRef Medline](#)
- Lee, J., Peña, M. M., Nose, Y., and Thiele, D. J. (2002) Biochemical characterization of the human copper transporter Ctr1. *J. Biol. Chem.* **277**, 4380–4387 [CrossRef Medline](#)
- Aller, S. G., and Unger, V. M. (2006) Projection structure of the human copper transporter CTR1 at 6-Å resolution reveals a compact trimer with a novel channel-like architecture. *Proc. Natl. Acad. Sci. U.S.A.* **103**, 3627–3632 [CrossRef Medline](#)
- De Feo, C. J., Aller, S. G., Siluvai, G. S., Blackburn, N. J., and Unger, V. M. (2009) Three-dimensional structure of the human copper transporter hCTR1. *Proc. Natl. Acad. Sci. U.S.A.* **106**, 4237–4242 [CrossRef Medline](#)
- Wu, X., Sinani, D., Kim, H., and Lee, J. (2009) Copper transport activity of yeast Ctr1 is down-regulated via its C terminus in response to excess copper. *J. Biol. Chem.* **284**, 4112–4122 [CrossRef Medline](#)
- Puig, S., Lee, J., Lau, M., and Thiele, D. J. (2002) Biochemical and genetic analyses of yeast and human high affinity copper transporters suggest a conserved mechanism for copper uptake. *J. Biol. Chem.* **277**, 26021–26030 [CrossRef Medline](#)
- Eisses, J. F., and Kaplan, J. H. (2005) The mechanism of copper uptake mediated by human CTR1: a mutational analysis. *J. Biol. Chem.* **280**, 37159–37168 [CrossRef Medline](#)
- Maryon, E. B., Molloy, S. A., Ivy, K., Yu, H., and Kaplan, J. H. (2013) Rate and regulation of copper transport by human copper transporter 1 (hCTR1). *J. Biol. Chem.* **288**, 18035–18046 [CrossRef Medline](#)
- Nose, Y., Wood, L. K., Kim, B. E., Prohaska, J. R., Fry, R. S., Spears, J. W., and Thiele, D. J. (2010) Ctr1 is an apical copper transporter in mammalian intestinal epithelial cells in vivo that is controlled at the level of protein stability. *J. Biol. Chem.* **285**, 32385–32392 [CrossRef Medline](#)
- Ohrvik, H., Nose, Y., Wood, L. K., Kim, B. E., Gleber, S. C., Ralle, M., and Thiele, D. J. (2013) Ctr2 regulates biogenesis of a cleaved form of mammalian Ctr1 metal transporter lacking the copper- and cisplatin-binding

CHCA-1-mediated copper homeostasis in worms

- ecto-domain. *Proc. Natl. Acad. Sci. U.S.A.* **110**, E4279–E4288 [CrossRef Medline](#)
15. Öhrvik, H., Logeman, B., Turk, B., Reinheckel, T., and Thiele, D. J. (2016) Cathepsin protease controls copper and cisplatin accumulation via cleavage of the Ctr1 metal-binding ectodomain. *J. Biol. Chem.* **291**, 13905–13916 [CrossRef Medline](#)
 16. Jungmann, J., Reins, H.-A., Lee, J., Romeo, A., Hassett, R., Kosman, D., and Jentsch, S. (1993) MAC1, a nuclear regulatory protein related to copper-dependent transcription factors is involved in Cu/Fe utilization and stress resistance in yeast. *EMBO J.* **12**, 5051–5056 [Medline](#)
 17. Zhou, H., Cadigan, K. M., and Thiele, D. J. (2003) A copper-regulated transporter required for copper acquisition, pigmentation, and specific stages of development in *Drosophila melanogaster*. *J. Biol. Chem.* **278**, 48210–48218 [CrossRef Medline](#)
 18. Mackenzie, N. C., Brito, M., Reyes, A. E., and Allende, M. L. (2004) Cloning, expression pattern and essentiality of the high-affinity copper transporter 1 (ctr1) gene in zebrafish. *Gene* **328**, 113–120 [CrossRef Medline](#)
 19. Kuo, Y.-M., Zhou, B., Cosco, D., and Gitschier, J. (2001) The copper transporter CTR1 provides an essential function in mammalian embryonic development. *Proc. Natl. Acad. Sci. U.S.A.* **98**, 6836–6841 [CrossRef Medline](#)
 20. Nose, Y., Kim, B. E., and Thiele, D. J. (2006) Ctr1 drives intestinal copper absorption and is essential for growth, iron metabolism, and neonatal cardiac function. *Cell Metab.* **4**, 235–244 [CrossRef Medline](#)
 21. Kim, B. E., Turski, M. L., Nose, Y., Casad, M., Rockman, H. A., and Thiele, D. J. (2010) Cardiac copper deficiency activates a systemic signaling mechanism that communicates with the copper acquisition and storage organs. *Cell Metab.* **11**, 353–363 [CrossRef Medline](#)
 22. Rao, A. U., Carta, L. K., Lesuisse, E., and Hamza, I. (2005) Lack of heme synthesis in a free-living eukaryote. *Proc. Natl. Acad. Sci. U.S.A.* **102**, 4270–4275 [CrossRef Medline](#)
 23. Korolnek, T., Zhang, J., Beardsley, S., Scheffer, G. L., and Hamza, I. (2014) Control of metazoan heme homeostasis by a conserved multidrug resistance protein. *Cell Metab.* **19**, 1008–1019 [CrossRef Medline](#)
 24. Davis, D. E., Roh, H. C., Deshmukh, K., Bruinsma, J. J., Schneider, D. L., Guthrie, J., Robertson, J. D., and Kornfeld, K. (2009) The cation diffusion facilitator gene *cdf-2* mediates zinc metabolism in *Caenorhabditis elegans*. *Genetics* **182**, 1015–1033 [CrossRef Medline](#)
 25. Anderson, C. P., and Leibold, E. A. (2014) Mechanisms of iron metabolism in *Caenorhabditis elegans*. *Front. Pharmacol.* **5**, 113 [Medline](#)
 26. Wakabayashi, T., Nakamura, N., Sambongi, Y., Wada, Y., Oka, T., and Futai, M. (1998) Identification of the copper chaperone, CUC-1, in *Caenorhabditis elegans*: tissue specific co-expression with the copper transporting ATPase, CUA-1. *FEBS Lett.* **440**, 141–146 [CrossRef Medline](#)
 27. Imagawa, M., Onozawa, T., Okumura, K., Osada, S., Nishihara, T., and Kondo, M. (1990) Characterization of metallothionein cDNAs induced by cadmium in the nematode *Caenorhabditis elegans*. *Biochem. J.* **268**, 237–240 [CrossRef Medline](#)
 28. Chun, H., Sharma, A. K., Lee, J., Chan, J., Jia, S., and Kim, B.-E. (2017) The intestinal copper exporter CUA-1 is required for systemic copper homeostasis in *Caenorhabditis elegans*. *J. Biol. Chem.* **292**, 1–14 [CrossRef Medline](#)
 29. Lee, J., Prohaska, J. R., Dagenais, S. L., Glover, T. W., and Thiele, D. J. (2000) Isolation of a murine copper transporter gene, tissue specific expression, and functional complementation of a yeast copper transport mutant. *Gene* **254**, 87–96 [CrossRef Medline](#)
 30. Petris, M. J., Smith, K., Lee, J., and Thiele, D. J. (2003) Copper-stimulated endocytosis and degradation of the human copper transporter, hCtr1. *J. Biol. Chem.* **278**, 9639–9646 [CrossRef Medline](#)
 31. Ooi, C. E., Rabinovich, E., Dancis, A., Bonifacino, J. S., and Klausner, R. D. (1996) Copper-dependent degradation of the *Saccharomyces cerevisiae* plasma membrane copper transporter Ctr1p in the apparent absence of endocytosis. *EMBO J.* **15**, 3515–3523 [Medline](#)
 32. Oka, T., Toyomura, T., Honjo, K., Wada, Y., and Futai, M. (2001) Four subunit isoforms of *Caenorhabditis elegans* vacuolar H⁺-ATPase. Cell-specific expression during development. *J. Biol. Chem.* **276**, 33079–33085 [CrossRef Medline](#)
 33. Mitani, S. (2009) Nematode, an experimental animal in the national BioResource project. *Exp. Anim.* **58**, 351–356 [CrossRef Medline](#)
 34. Qadota, H., Inoue, M., Hikita, T., Köppen, M., Hardin, J. D., Amano, M., Moerman, D. G., and Kaibuchi, K. (2007) Establishment of a tissue-specific RNAi system in *C. elegans*. *Gene* **400**, 166–173 [CrossRef Medline](#)
 35. Maryon, E. B., Molloy, S. A., and Kaplan, J. H. (2007) O-Linked glycosylation at threonine 27 protects the copper transporter hCTR1 from proteolytic cleavage in mammalian cells. *J. Biol. Chem.* **282**, 20376–20387 [CrossRef Medline](#)
 36. Sambongi, Y., Nagae, T., Liu, Y., Yoshimizu, T., Takeda, K., Wada, Y., and Futai, M. (1999) Sensing of cadmium and copper ions by externally exposed ADL, ASE, and ASH neurons elicits avoidance response in *Caenorhabditis elegans*. *Neuroreport* **10**, 753–757 [CrossRef Medline](#)
 37. Guo, M., Wu, T.-H., Song, Y.-X., Ge, M.-H., Su, C.-M., Niu, W.-P., Li, L.-L., Xu, Z.-J., Ge, C.-L., Al-Mhanawi, M. T., Wu, S. P., and Wu, Z. X. (2015) Reciprocal inhibition between sensory ASH and ASI neurons modulates nociception and avoidance in *Caenorhabditis elegans*. *Nat. Commun.* **6**, 5655 [CrossRef Medline](#)
 38. Hao, L., Efimenko, E., Swoboda, P., and Scholey, J. M. (2011) The retrograde IFT machinery of *C. elegans* cilia: two IFT dynein complexes? *PLoS ONE* **6**, e20995 [CrossRef Medline](#)
 39. Bousquet-Moore, D., Mains, R. E., and Eipper, B. A. (2010) Peptidylglycine α -amidating monooxygenase and copper: A gene–nutrient interaction critical to nervous system function. *J. Neurosci. Res.* **88**, 2535–2545 [CrossRef Medline](#)
 40. Calixto, A., Chelur, D., Topalidou, I., Chen, X., and Chalfie, M. (2010) Enhanced neuronal RNAi in *C. elegans* using SID-1. *Nat. Methods* **7**, 554–559 [CrossRef Medline](#)
 41. Husson, S. J., Janssen, T., Baggerman, G., Bogert, B., Kahn-Kirby, A. H., Ashrafi, K., and Schoofs, L. (2007) Impaired processing of FLP and NLP peptides in carboxypeptidase E (EGL-21)-deficient *Caenorhabditis elegans* as analyzed by mass spectrometry. *J. Neurochem.* **102**, 246–260 [CrossRef Medline](#)
 42. Kass, J., Jacob, T. C., Kim, P., and Kaplan, J. M. (2001) The EGL-3 proprotein convertase regulates mechanosensory responses of *Caenorhabditis elegans*. *J. Neurosci.* **21**, 9265–9272 [CrossRef Medline](#)
 43. Beaudoin, J., Thiele, D. J., Labbé, S., and Puig, S. (2011) Dissection of the relative contribution of the *Schizosaccharomyces pombe* Ctr4 and Ctr5 proteins to the copper transport and cell surface delivery functions. *Microbiology* **157**, 1021–1031 [CrossRef Medline](#)
 44. Roh, H. C., Collier, S., Guthrie, J., Robertson, J. D., and Kornfeld, K. (2012) Lysosome-related organelles in intestinal cells are a zinc storage site in *C. elegans*. *Cell Metab.* **15**, 88–99 [CrossRef Medline](#)
 45. Gourley, B. L., Parker, S. B., Jones, B. J., Zumbrennen, K. B., and Leibold, E. A. (2003) Cytosolic aconitase and ferritin are regulated by iron in *Caenorhabditis elegans*. *J. Biol. Chem.* **278**, 3227–3234 [CrossRef Medline](#)
 46. Chen, C., Samuel, T. K., Krause, M., Dailey, H. A., and Hamza, I. (2012) Heme utilization in the *Caenorhabditis elegans* hypodermal cells is facilitated by heme-responsive gene-2. *J. Biol. Chem.* **287**, 9601–9612 [CrossRef Medline](#)
 47. Mak, H. Y. (2012) Lipid droplets as fat storage organelles in *Caenorhabditis elegans* thematic review series: lipid droplet synthesis and metabolism: from yeast to man. *J. Lipid Res.* **53**, 28–33 [CrossRef Medline](#)
 48. Aoki, I., and Mori, I. (2015) Molecular biology of thermosensory transduction in *C. elegans*. *Curr. Opin. Neurobiol.* **34**, 117–124 [CrossRef Medline](#)
 49. Bretscher, A. J., Busch, K. E., and de Bono, M. (2008) A carbon dioxide avoidance behavior is integrated with responses to ambient oxygen and food in *Caenorhabditis elegans*. *Proc. Natl. Acad. Sci. U.S.A.* **105**, 8044–8049 [CrossRef Medline](#)
 50. Bretscher, A. J., Kodama-Namba, E., Busch, K. E., Murphy, R. J., Soltesz, Z., Laurent, P., and de Bono, M. (2011) Temperature, oxygen, and salt-sensing neurons in *C. elegans* are carbon dioxide sensors that control avoidance behavior. *Neuron* **69**, 1099–1113 [CrossRef Medline](#)
 51. Bargmann, C. I., Hartwig, E., and Horvitz, H. R. (1993) Odorant-selective genes and neurons mediate olfaction in *C. elegans*. *Cell* **74**, 515–527 [CrossRef Medline](#)

52. Zhang, Y., Lu, H., and Bargmann, C. I. (2005) Pathogenic bacteria induce aversive olfactory learning in *Caenorhabditis elegans*. *Nature* **438**, 179–184 [CrossRef Medline](#)
53. Hilliard, M. A., Apicella, A. J., Kerr, R., Suzuki, H., Bazzicalupo, P., and Schafer, W. R. (2005) *In vivo* imaging of *C. elegans* ASH neurons: cellular response and adaptation to chemical repellents. *EMBO J.* **24**, 63–72 [CrossRef Medline](#)
54. Du, M., and Wang, D. (2009) The neurotoxic effects of heavy metal exposure on GABAergic nervous system in nematode *Caenorhabditis elegans*. *Environ. Toxicol. Pharmacol.* **27**, 314–320 [CrossRef Medline](#)
55. Block, E., Batista, V. S., Matsunami, H., Zhuang, H., and Ahmed, L. (2017) The role of metals in mammalian olfaction of low molecular weight organosulfur compounds. *Nat. Prod. Rep.* **34**, 529–557 [CrossRef Medline](#)
56. Frooninckx, L., Van Rompay, L., Temmerman, L., Van Sinay, E., Beets, I., Janssen, T., Husson, S. J., and Schoofs, L. (2012) Neuropeptide GPCRs in *C. elegans*. *Front. Endocrinol.* **3**, 167 [CrossRef Medline](#)
57. Li, C., and Kim, K. (2008) Neuropeptides. *WormBook 2008*, 1–36 [CrossRef Medline](#)
58. Brenner, S. (1974) The genetics of *Caenorhabditis elegans*. *Genetics* **77**, 71–94 [Medline](#)
59. Yuan, X., Protchenko, O., Philpott, C. C., and Hamza, I. (2012) Topologically conserved residues direct heme transport in HRG-1-related proteins. *J. Biol. Chem.* **287**, 4914–4924 [CrossRef Medline](#)
60. Kamath, R. S., Fraser, A. G., Dong, Y., Poulin, G., Durbin, R., Gotta, M., Kanapin, A., Le Bot, N., Moreno, S., Sohrmann, M., Welchman, D. P., Zipperlen, P., and Ahringer, J. (2003) Systematic functional analysis of the *Caenorhabditis elegans* genome using RNAi. *Nature* **421**, 231–237 [CrossRef Medline](#)
61. Rual, J.-F., Ceron, J., Koreth, J., Hao, T., Nicot, A.-S., Hirozane-Kishikawa, T., Vandenhaute, J., Orkin, S. H., Hill, D. E., van den Heuvel, S., and Vidal, M. (2004) Toward improving *Caenorhabditis elegans* phenome mapping with an ORFeome-based RNAi library. *Genome Res.* **14**, 2162–2168 [CrossRef Medline](#)
62. Anderson, J. L., Morran, L. T., and Phillips, P. C. (2010) Outcrossing and the maintenance of males within *C. elegans* populations. *J. Hered.* **101**, Suppl. 1, S62–S74 [CrossRef Medline](#)
63. Finney, M., and Ruvkun, G. (1990) The unc-86 gene product couples cell lineage and cell identity in *C. elegans*. *Cell* **63**, 895–905 [CrossRef Medline](#)